We are IntechOpen,
the world's leading publisher of
Open Access books
Built by scientists, for scientists

5,000
Open access books available

125,000
International authors and editors

140M
Downloads

Our authors are among the

154
Countries delivered to

TOP 1%
most cited scientists

12.2%
Contributors from top 500 universities

Interested in publishing with us?
Contact book.department@intechopen.com

Numbers displayed above are based on latest data collected.
For more information visit www.intechopen.com

Applications of Diffusion Hydrodynamic Model

Theodore V. Hromadka II and Chung-Cheng Yen

Abstract

The diffusion hydrodynamic model is applied for seven engineering applications that are commonly encountered in real-world applications. Of the seven applications, six relate to two-dimensional flows. The results are compared to other model results, where available. The results underscore the reliability of the DHM along with its limitation for modeling rapidly varying flows.

Keywords: hydraulic jump, hydrograph, two-dimensional flows, estuary, channel flood plain interface

1. One-dimensional model application

1.1 Application 1: steady flow in an open channel

Because the DHM is anticipated for use in modeling watershed phenomena, it is important that the channel models represent known flow characteristics. Unsteady flow is examined in the previous section. For steady flow, a steady-state, gradually varied flow problem is simulated by the 2-D diffusion model. **Figure 1** depicts both the water levels form the 2-D diffusion model and from the gradually varied flow equation. For an 8000 cfs constant inflow rate, the water surface profiles from both the 2-D diffusion model and the gradually varied flow equation match quite well. The discrepancies of these profiles occur at the breakpoints where the upstream channel slope and downstream channel slope change. At the first break point where the upstream channel slope is equal to 0.001 and the downstream channel slope is equal to 0.005, the water surface level is assumed to be equal to the critical depth. However, Henderson [1] notes that brink flow is typically less than the critical depth (Dc). The DHM water surface closely matches the 0.72 Dc brink depth.

It is clear to see that the DHM cannot simulate the hydraulic jump but rather smooth out the usually assumed "shock front." However, when considering unsteady flow, the DHM may be a reasonable approach for approximating the jump profile. For a higher inflow rate, 20,000 cfs, the surface water levels differ in the most upstream reach. Again, this is due to the downstream control, critical depth, of the gradually varied flow equation.
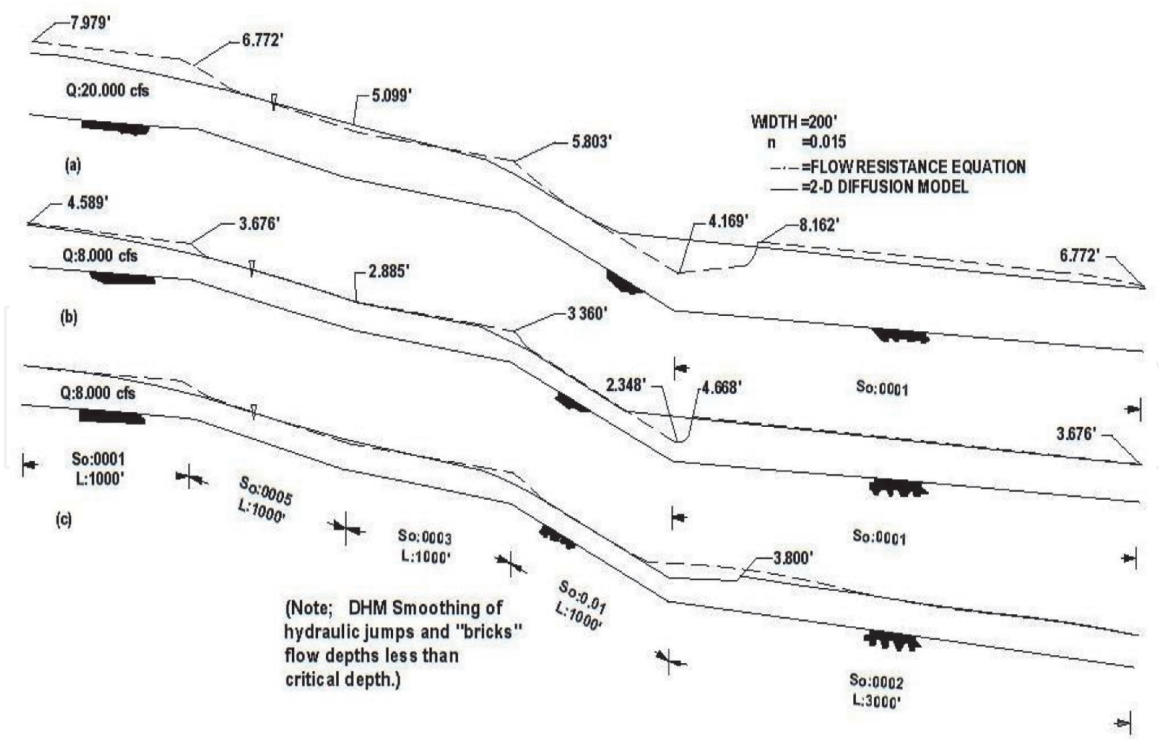
Figure 1.
Gradually varied flow profiles. (a) Q = 20,000 cfs, downstream slope = 0.0001 (b) Q = 8,000 cfs, downstream slope = 0.0001 (c) Q = 8,000 cfs, downstream slope = 0.0002.

2. Two-dimensional model applications

2.1 Application 2: rainfall-runoff model

The DHM can be used to develop a runoff hydrograph given the time distribution of effective rainfall. To demonstrate the DHM runoff hydrograph generation [2], the DHM is used to develop a synthetic S-graph for a watershed where the overland flow is the dominating flow effect.

To develop the S-graph, a uniform effective rainfall is assumed to uniformly occur over the watershed. For each time step (5 s), an incremental volume of water is added directly to each grid element based on the assumed constant rainfall intensity, resulting in an equivalent increase in the nodal point depth of water. Runoff flows to the point of concentration according to the two-dimensional diffusion hydrodynamics model.

The 10 square mile Cucamonga Creek Watershed (California) is shown, discretized by 1000-foot grid elements, in **Figure 2**. A design storm (**Figure 3**) was applied to the watershed, and the resulting runoff hydrographs are depicted in **Figure 4** for DHM and synthetic unit hydrograph method. From **Figure 4**, the diffusion model generates runoff quantities which are in good agreement with the values computed using a synthetic unit hydrograph method derived from stream gage data.

Next, the DHM is applied to three hypothetical dam failures in Orange County, California (see **Figure 5**). In this application, the ability of DHM to predict flow characteristics in domains where flood flow patterns are affected by railroad, the bridge under crossings, and other man-made obstacles to flow is illustrated.
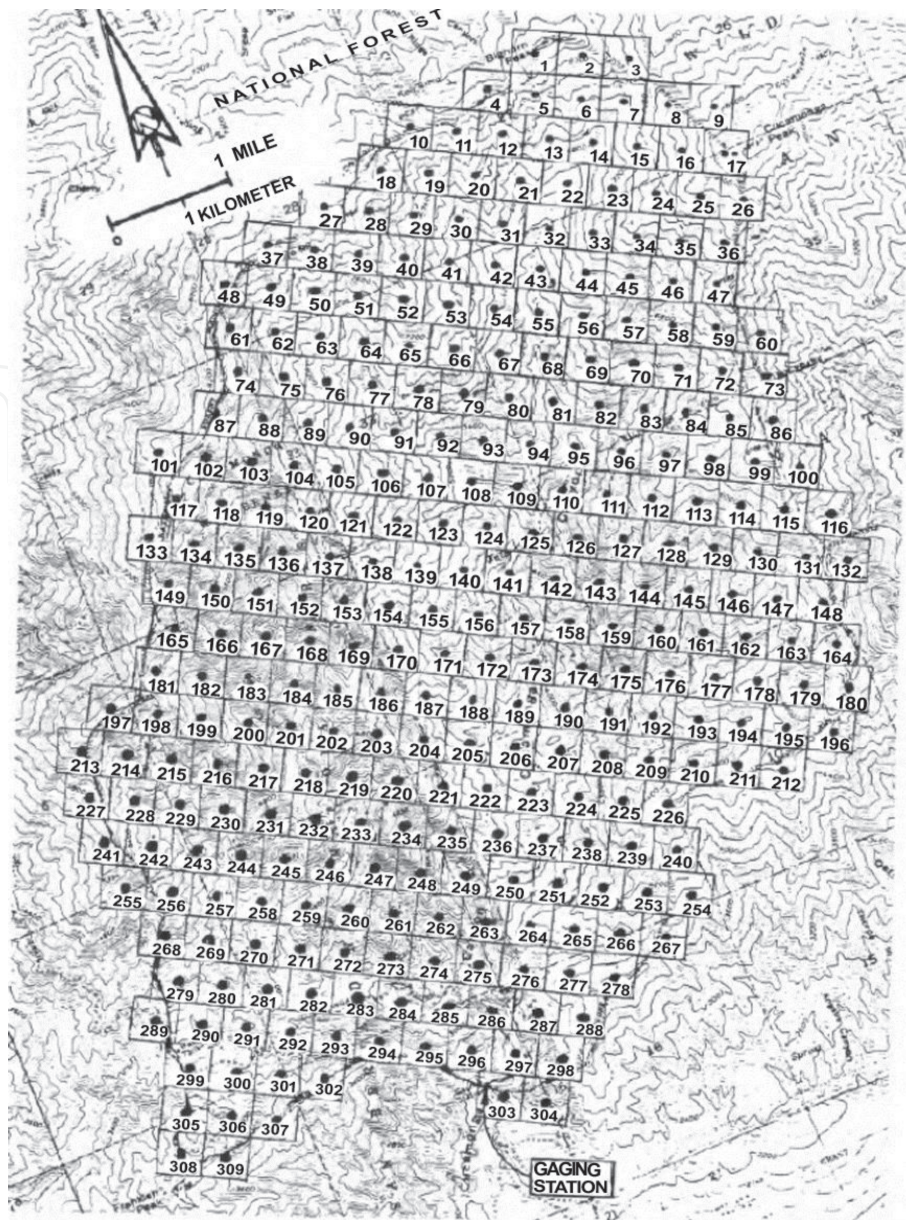
Figure 2.
Cucamonga Creek discretization.

Major assumptions used in these assumptions are as follows:

1. In each grid, an area-averaged ground elevation was estimated based on the topographic map, and a Manning's roughness coefficient was used for each application.

2. All storm drain systems provide negligible draw off of the dam-break flows. This assumption accommodates a design storm in progress during the dam failure. This assumption also implies that stormwater runoff provides a negligible increase to the dam-break flow hydrograph.

3. All canyon damming effects due to culvert crossings provide negligible attenuation of dam-break flows. This assumption is appropriate due to the concurrent design storm assumption and due to sediment deposition from the transport of the reservoir earthen dam materials.

4. The reservoir failure yields an outflow hydrograph, as depicted in **Figure 6**.

3
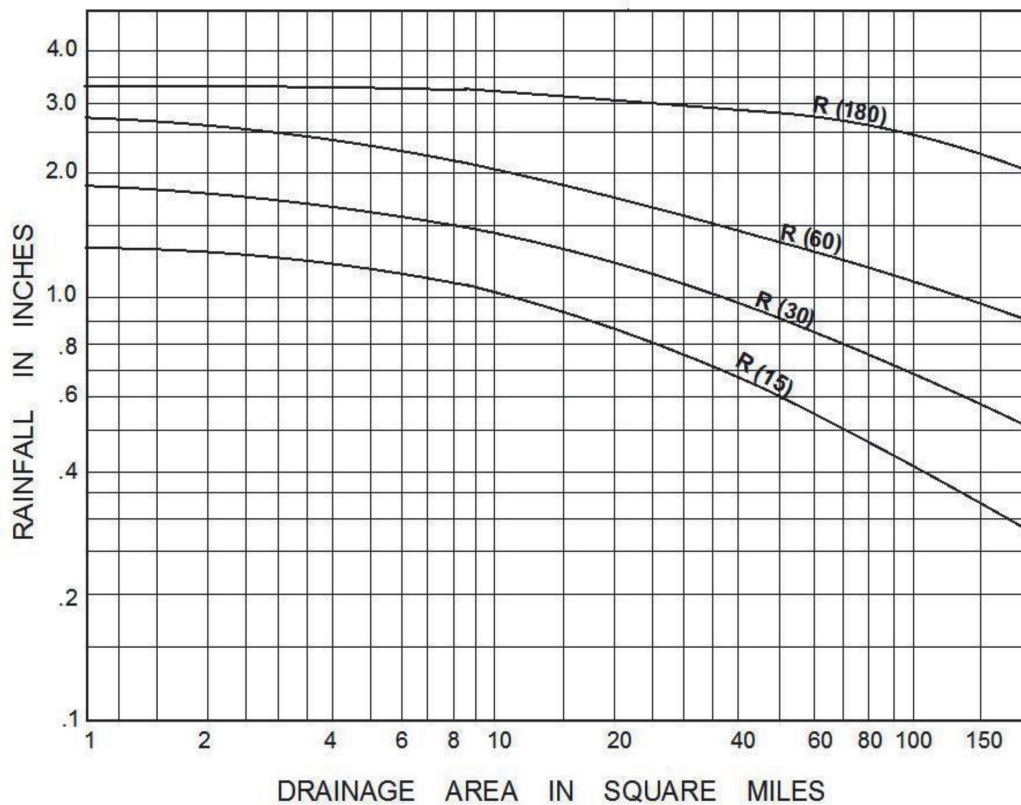
HYETOGRAPH COMPUTATION

UNIT PERIOD	AMOUNT	
1	.07	(R(180)-R(60))
2	.05	(R(180)-R(60))
3	.11	(R(180)-R(60))
4	.05	(R(180)-R(60))
5	.20	(R(180)-R(60))
6	.22	(R(180)-R(60))
7	.14	(R(180)-R(60))
8	.16	(R(180)-R(60))
9	.48	(R(60)-R(30))
10	.52	(R(60)-R(30))
11	1.00	(R(15))
12	1.00	(R(30)-R(15))

Note:
R(15) - Rainfall (inches) in 15 minute curation

LOCAL PROJECT STORM
DEPTH AREA DURATION CURVES

Figure 3.
Design storm for Cucamonga Creek.

2.2 Application 3: small dam-break floodplain analysis

A study of a hypothetical failure of the Orange Country Reservoir northeast of the city of Brea, California (**Figure 7**), was conducted by Hromadka and Lai [3]. Using the USGS topographic quadrangle map (photo-revised, 1981), a 500-foot grid discretization was prepared (**Figure 8**), and nodal-area ground elevations were estimated based on the map. A Manning's roughness coefficient of n = 0.040 was used throughout the study, except in canyon reaches and grassy plains, where n was selected as 0.030 and 0.050, respectively. In this study, the resulting flood plain and the comparison of the model-simulated flood plain to a previous study by the Metropolitan Water District of Southern California [4] are shown in **Figure 9**. The main difference in the estimated flood plains is due to the dynamic nature of the
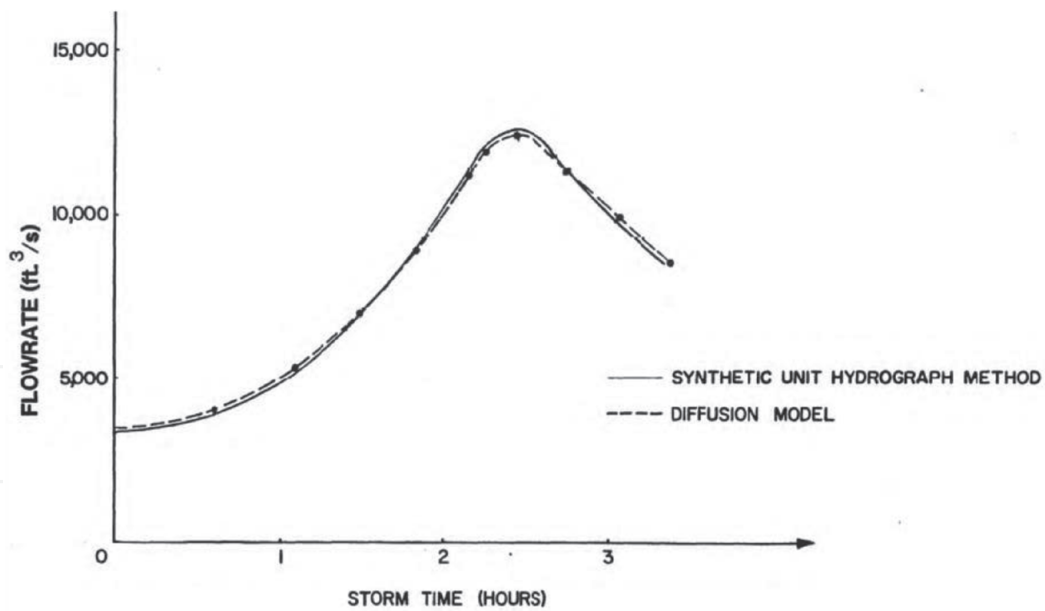
Figure 4.
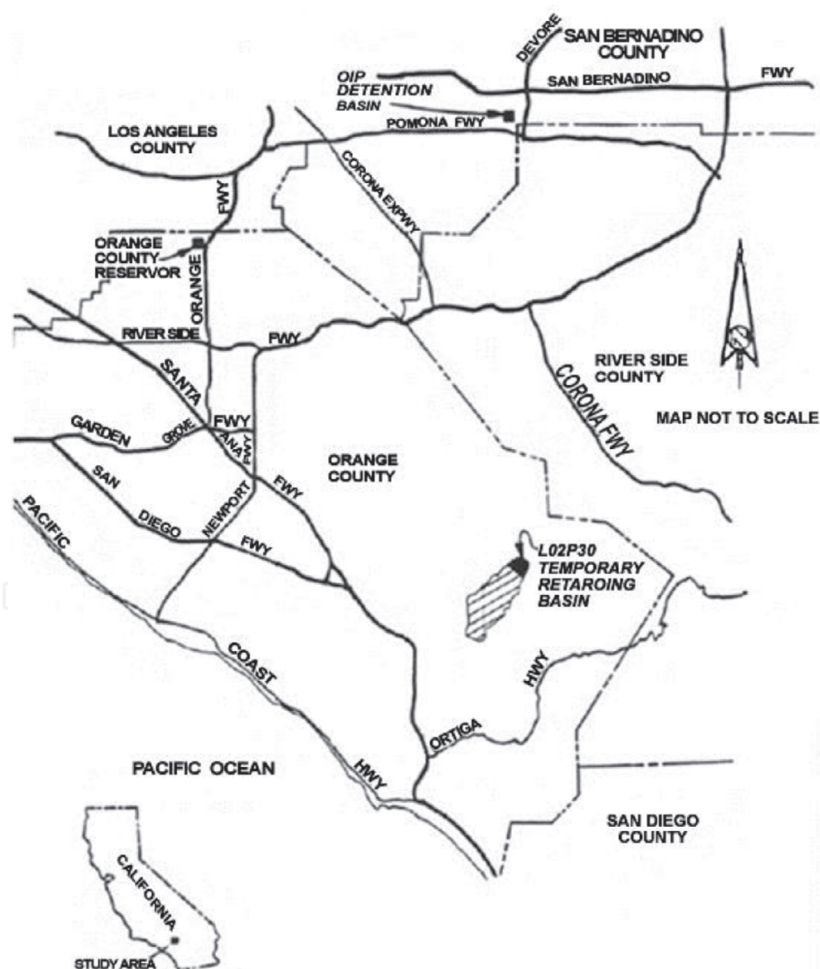*Simulated runoff hydrographs for Cucamonga Creek.*

Figure 5.
Vicinity map for dam-break analyses.

DHM, which accounts for the storage effects resulting from flooding, and the attenuation of a flood wave because of 2-D routing effects. From this study, the estimated flood plain is judged to be reasonable.
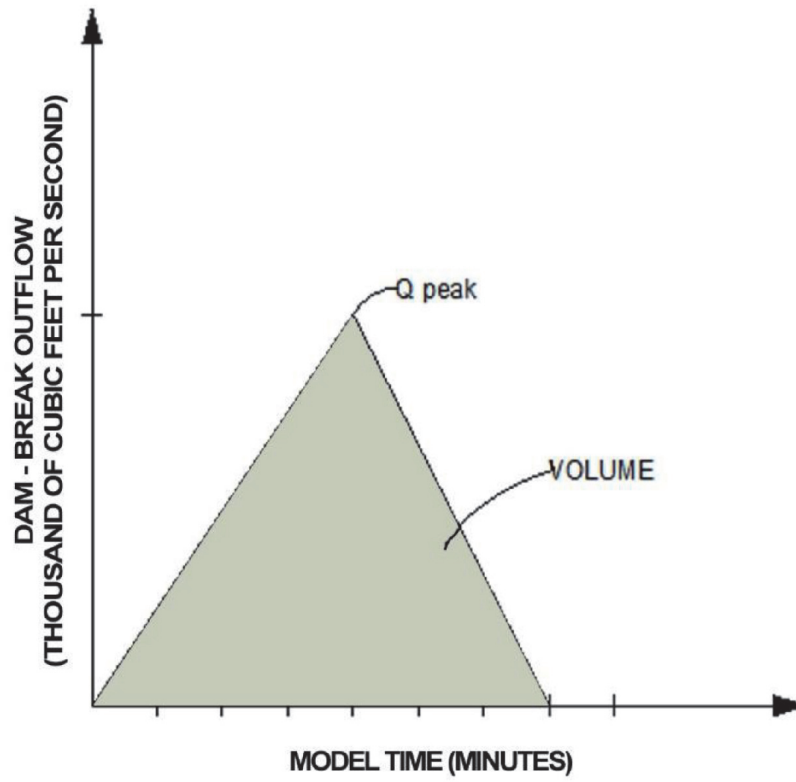
Figure 6.
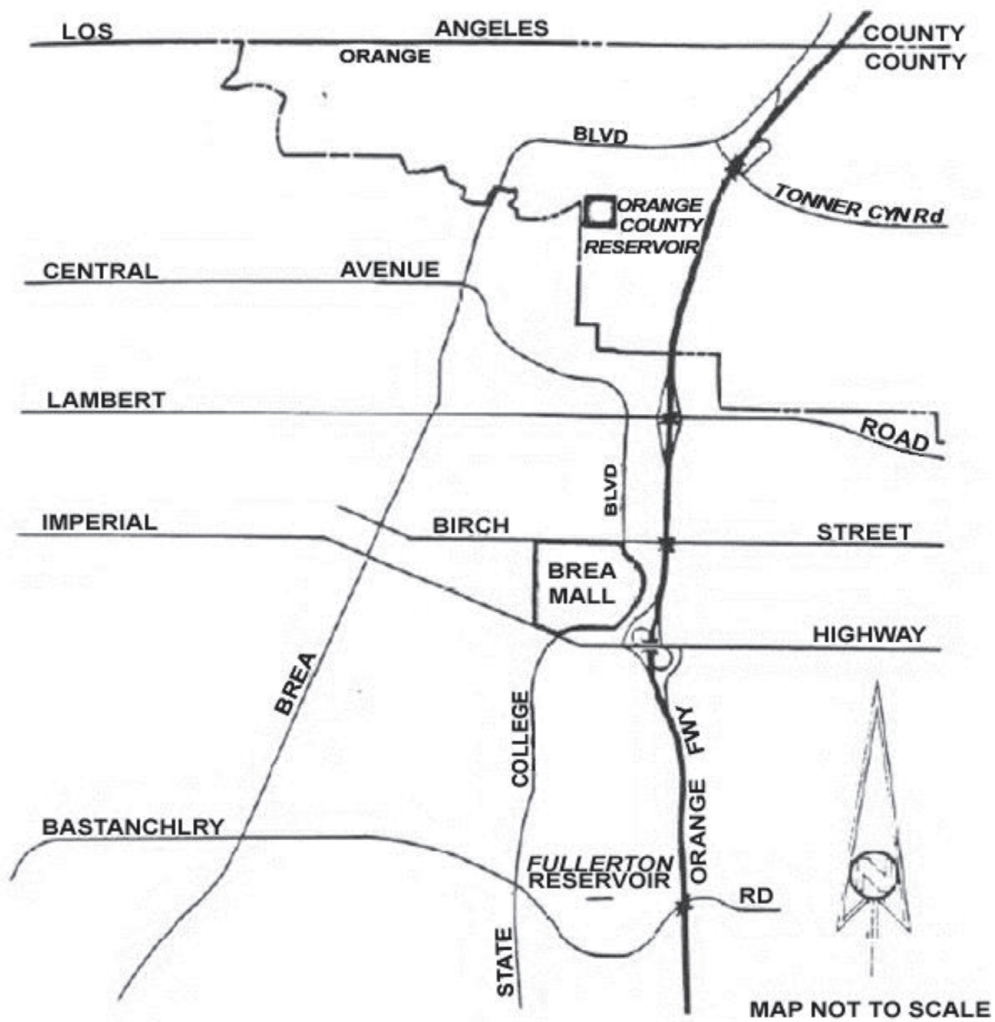*Study dam-break outflow hydrograph for Orange County Reservoir.*

Figure 7.
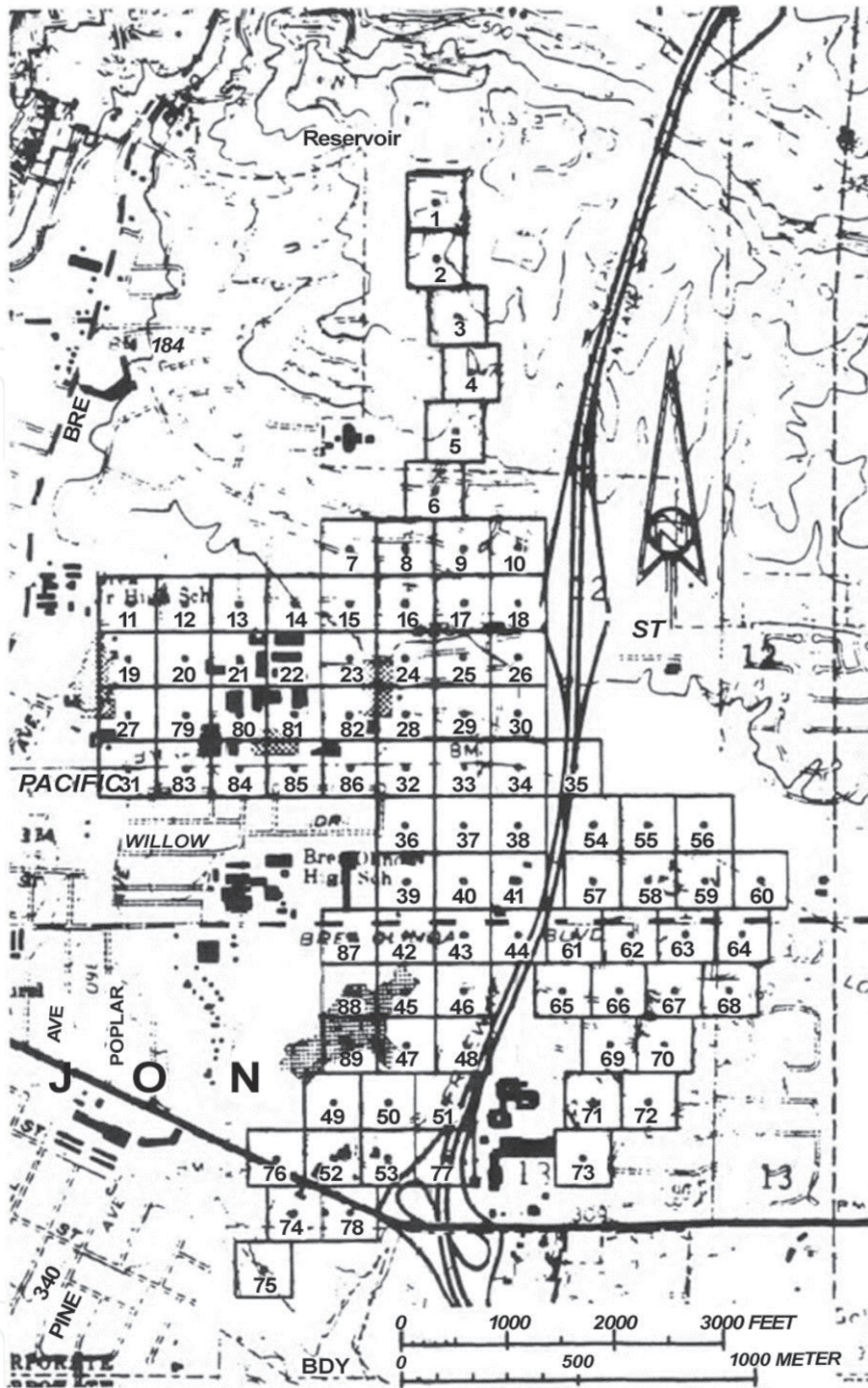*Location map for the Orange County Reservoir dam-break problem.*

Figure 8.
Domain discretization for Orange County Reservoir.

2.3 Application 4: small-scale flows onto a flat plain

A common civil engineering problem is the use of temporary detention basins to offset the effects of urbanization on watershed runoff. A problem, however, is the analysis of the basin failure, especially, when the flood flows enter a wide expanse of land surface with several small channels. This application is to present study conclusions in estimating the flood plain, which may result from a hypothetical dam failure of the LO2P3O temporary retarding basin. The results of this study are to be used to estimate the potential impacts of the area if the retention basin berm were to fail.

The study site includes the area south of Plano Trabuco, Phase I. It is bounded on the north of LO2P3O Retarding Basin Berm, on the east and
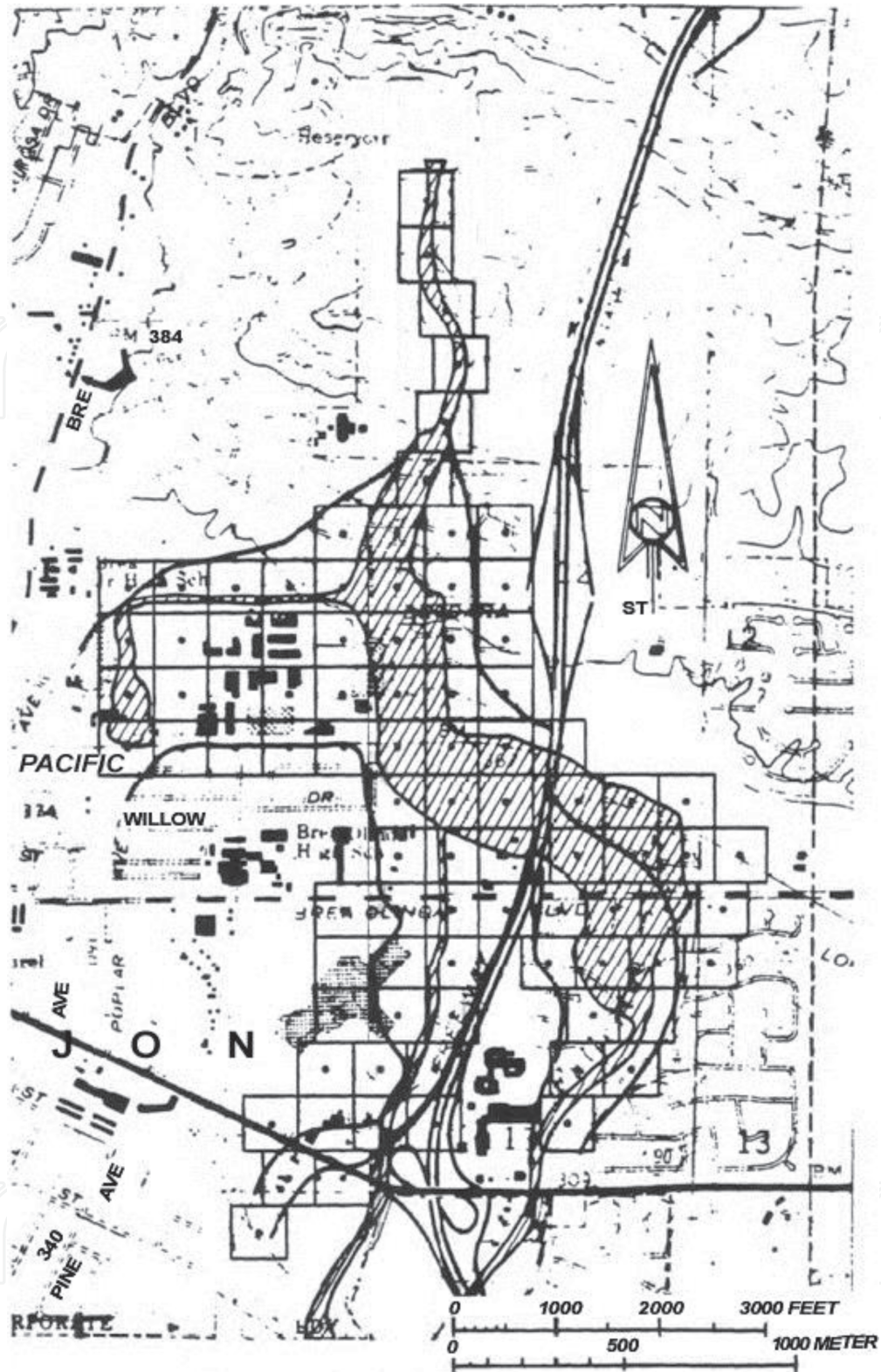
Figure 9.
Comparison of flood plain results for Orange County Reservoir.

south of Portola Parkway, and on the west by the Arroyo Trabuco bluffs (see **Figure 10**).

Using a 1″ = 300′ topographic map, a 200-foot grid control volume discretization was constructed, as shown in **Figure 11**. In each grid, an area-averaged ground elevation was estimated based on the topographic map. A Manning's roughness coefficient of n = 0.030 was used throughout the study.
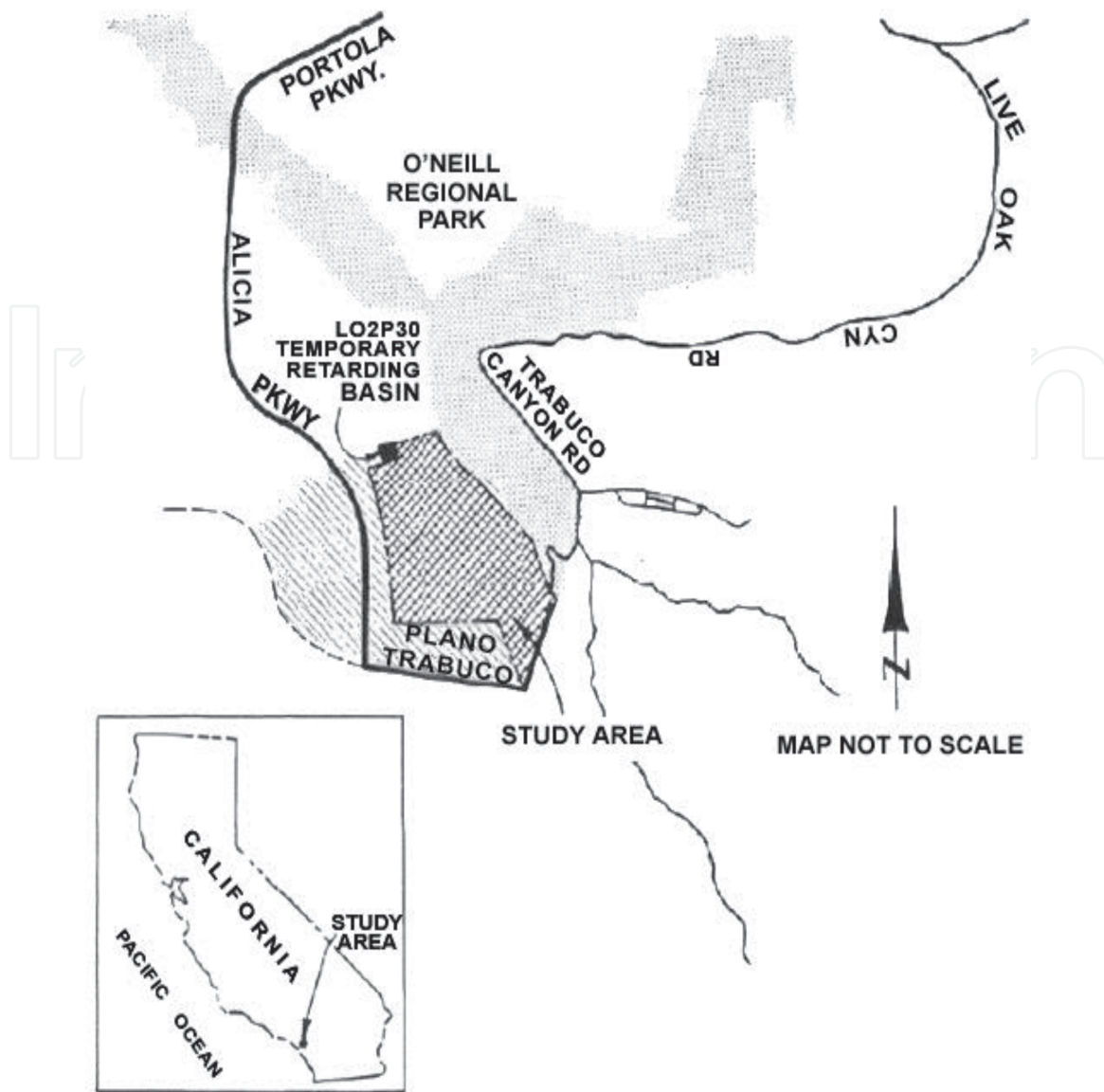
Figure 10.
Location map for L02P30 temporary retarding basin.

The profile of Portola Parkway varies approximately 2 ft above and below the adjacent land. Consequently, minor ponding may occur where Portola Parkway is high and sheet flow across Portola Parkway will occur at low points. It should be noted that depths along Portola Parkway are less than 1 foot (**Figure 11**). **Figure 12** shows lines of arrival times for the basin study. It is concluded that Portola Parkway is essentially unaffected by a hypothetical failure of the LO2P3O temporary retarding basin.

2.4 Application 5: two-dimensional flood flows around a large obstruction

In another temporary detention basin site, flood flows (from a dam-break) would pond upstream of a landfill site, and then split, when waters are deep enough, to flow on either side of the landfill. An additional complication is a railroad berm located downstream of the landfill, which forms a channel for flood flows. The study site (see **Figure 13**) is bounded on the north by a temporary berm approximately 300 ft north of the Union Pacific Railroad, bounded on the east by Milliken Avenue, bounded on the south by the Union Pacific Railroad, and bounded on the west by Haven Avenue.
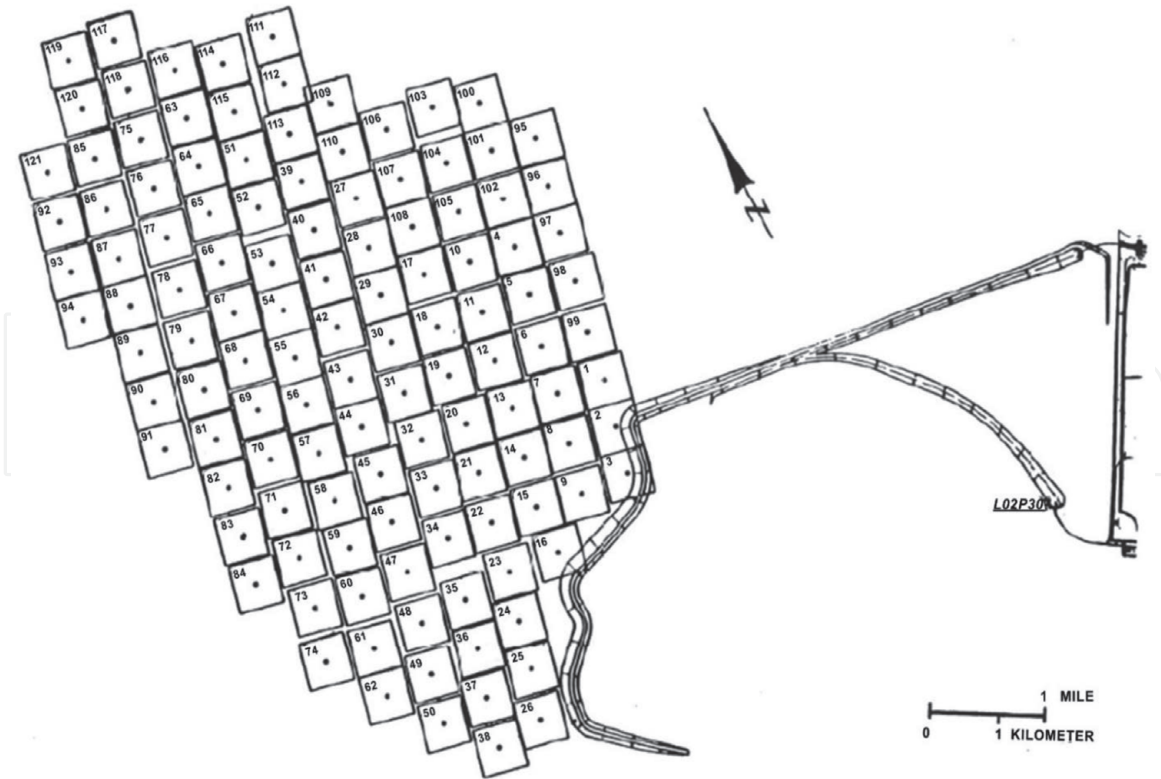
Figure 11.
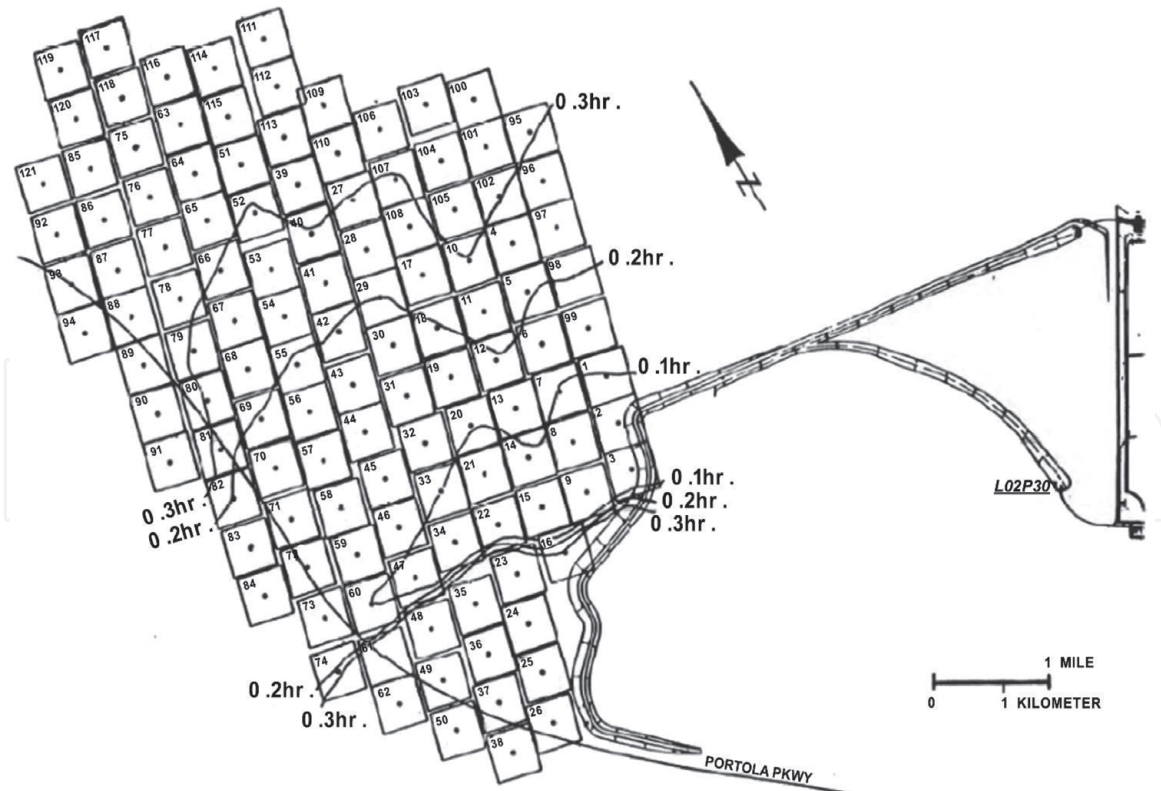*Domain discretization of L02P30 temporary retarding basin.*

Figure 12.
Time of maximum flooding depth (80.5 acre—Feet basin test) for L02P30 temporary retarding basin.

A 200-foot grid control volume discretization was constructed as depicted in **Figure 14**. In each grid, an area-averaged ground elevation was estimated based on the topographic map. A Manning's roughness coefficient of n = 0.030 was used throughout the study.

Figure 13.
Location map for Ontario industrial partners' temporary detention basin.
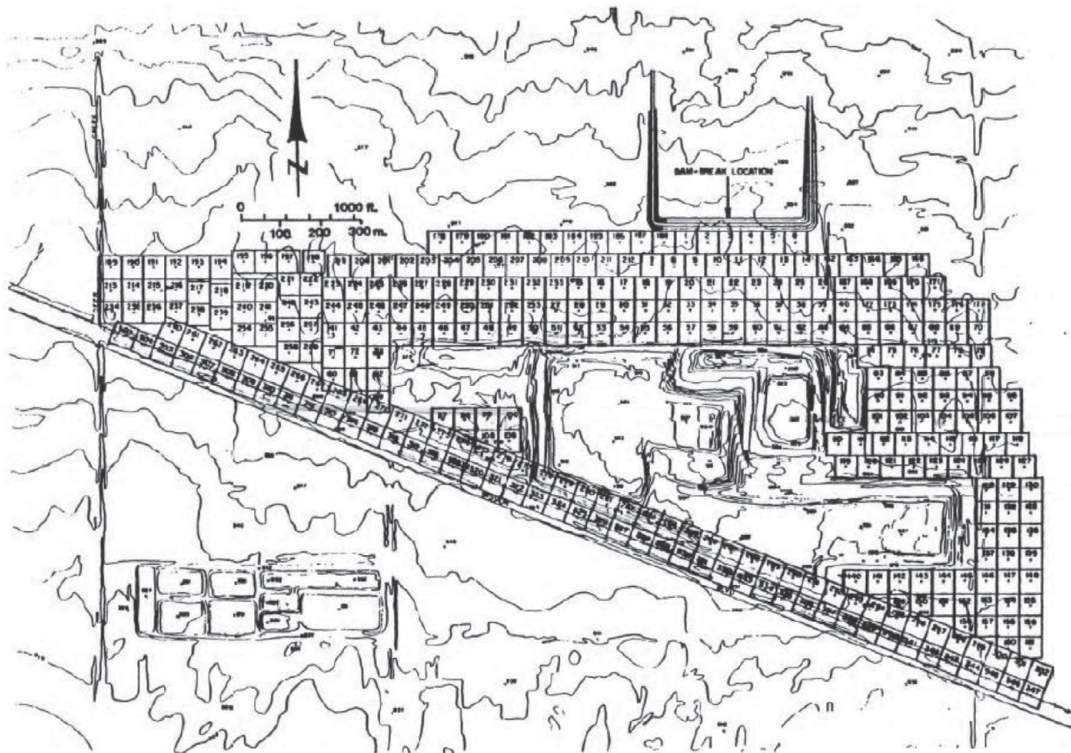
Figure 14.
Domain discretization for Ontario industrial partners' detention basin.

From **Figure 15**, it is seen that flood plain spreads out laterally and flows around the landfill. The flow ponds up around the landfill; along the north side of the landfill, the water ponds as high as 9.2 ft, and along the east and west sides of the
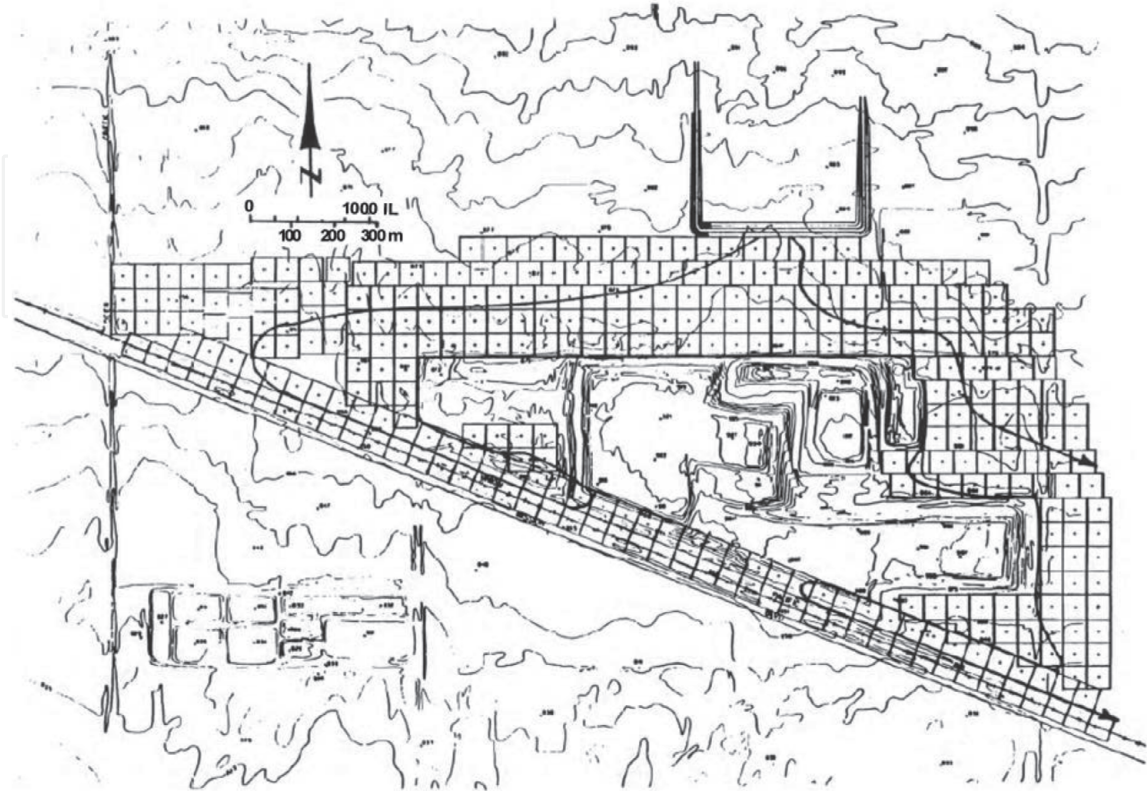
Figure 15.
Flood plain for Ontario industrial partners' detention basin.
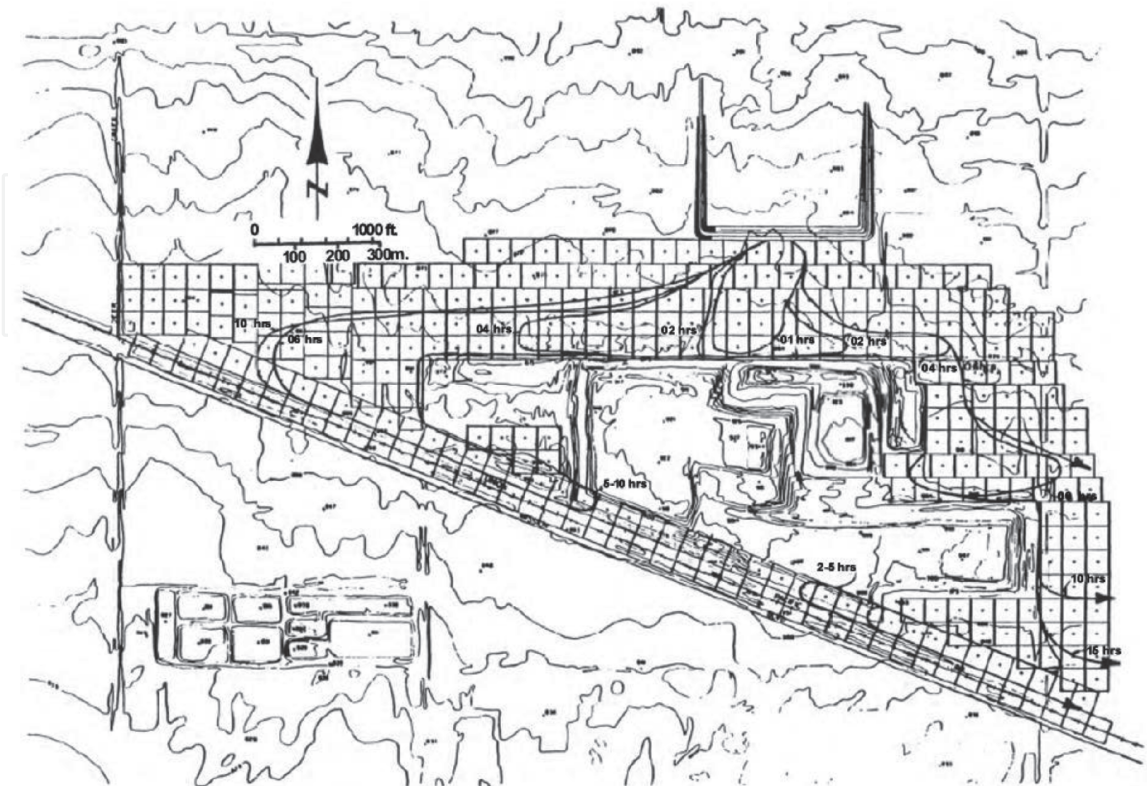
Figure 16.
Time (h) of maximum flooding depth for Ontario industrial partners detention basin.

landfill, the water ponds up to 5.1 ft high. As the flow travels south, it ponds up to a depth of 4.8 ft against the railroad near Milliken Avenue. Because the water spreads laterally, Milliken Avenue runs the risk of becoming flooded; however, the water only ponds to 0.6 ft along the street. A more in-depth study is needed to see if the water would remain in the gutter or flood Milliken Avenue.

By observing the arrival times of the flood plain in **Figure 16**, it is seen that the flood plain changes very little on the west side of the landfill once it reaches the railroad (0.6 h after the dam-break). But on the east side of the landfill, it takes 2.0 h to reach the railroad.
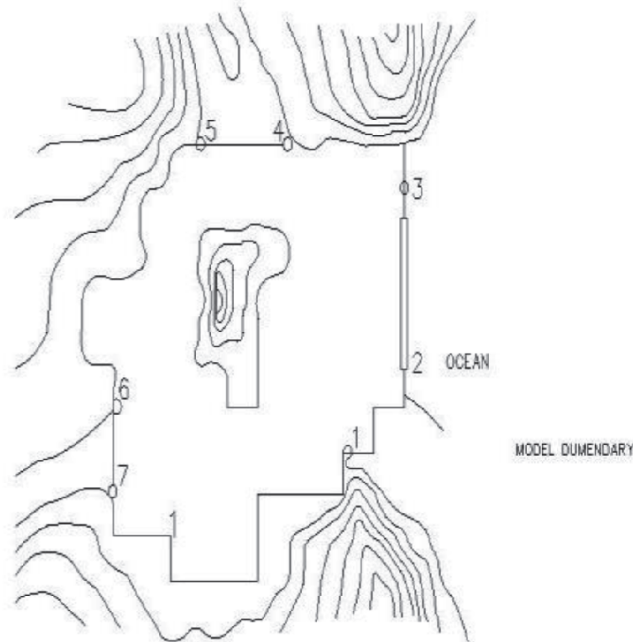
Figure 17.
A hypothetical bay.
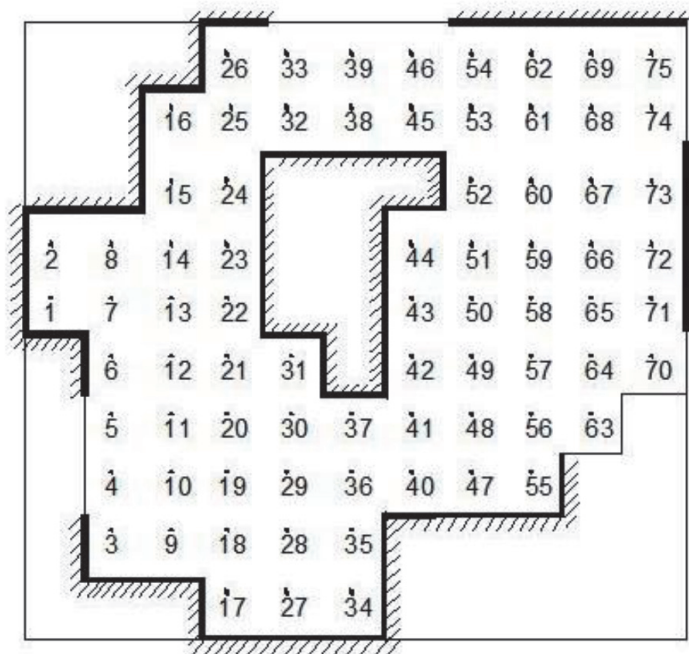
Figure 18.
The schematization of a hypothetical bay shown in **Figure 17**.

Boundary value equation: $z = a \sin\left[\frac{2\pi(t-\xi)}{T}\right] + M + 100$			
in which			
a = amplitude, and t = time (s)			
ξ = phase lag, and T = tidal period = 12.4 h = 44640 s			
M = mean water level			
NODE	**a (ft)**	**ξ (sec)**	**M (ft)**
63	5	0	0
70	4.95	60	0
74	4.85	180	0
75	4.85	180	0
46	4.75	1200	0.3
39	4.725	1260	0.35
33	4.7	1320	0.4
5	4.5	1800	0.7
4	4.45	1860	0.75

Table 1.
Boundary values for flow computation in a hypothetical bay.

2.5 Application 6: estuary modeling

Figure 17 illustrates a hypothetical bay, which is schematized in **Figure 18**. Stage hydrographs are available at seven stations as marked in **Figure 17** and are numbered 1–7 (counterclockwise). Stage values in this application are expressed by sinusoidal equations (see **Table 1**). Some DHM-predicted flow patterns in the estuary are shown in **Figures 19–21**. The flow patterns appear reasonable by comparing the fluctuations of the water surface to the stage
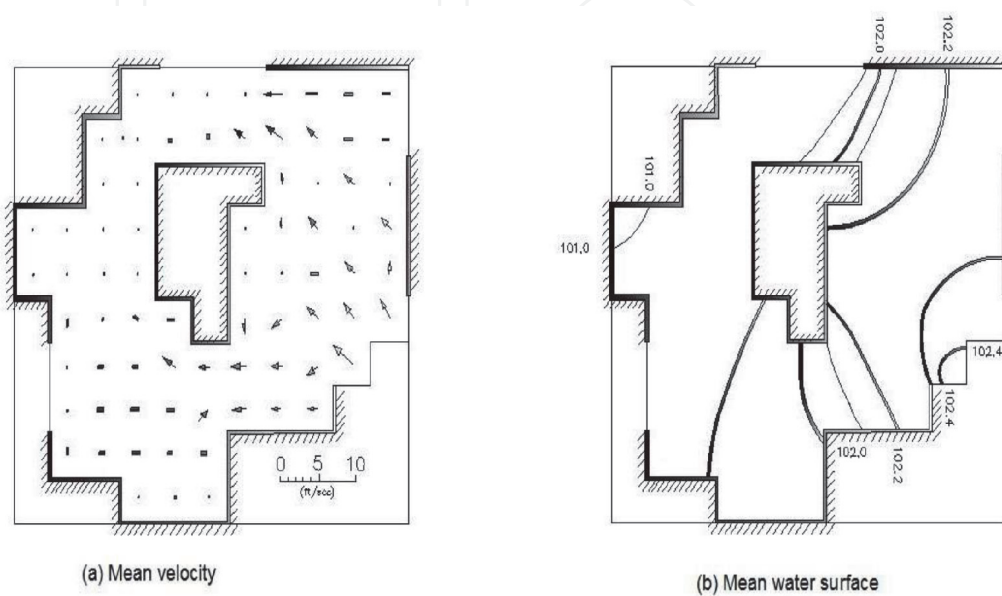

(a) Mean velocity

(b) Mean water surface

Figure 19.
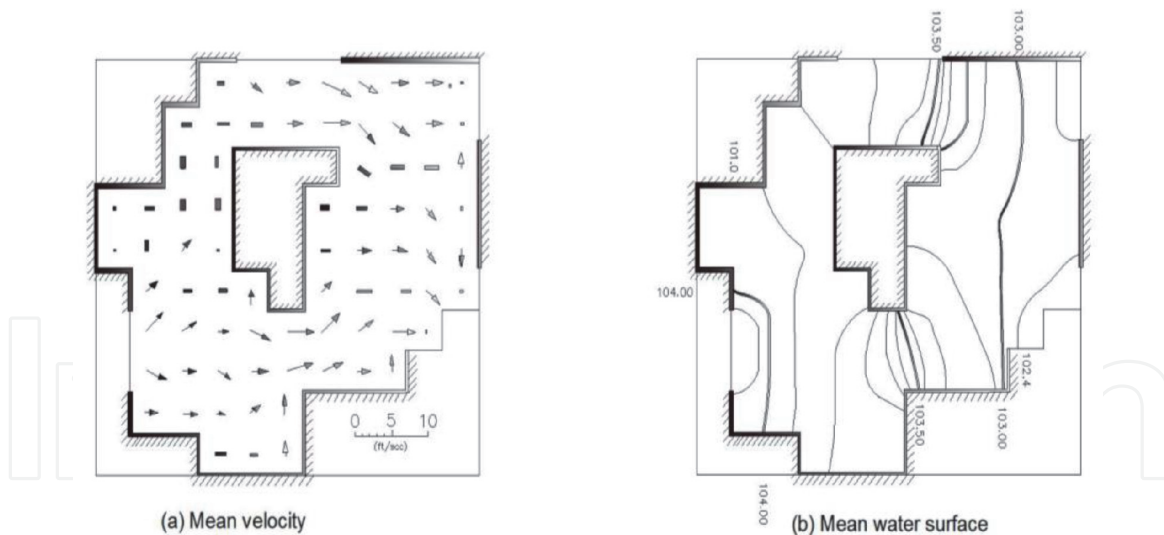*Mean velocity and water surface profiles at 1 h.*

Figure 20.
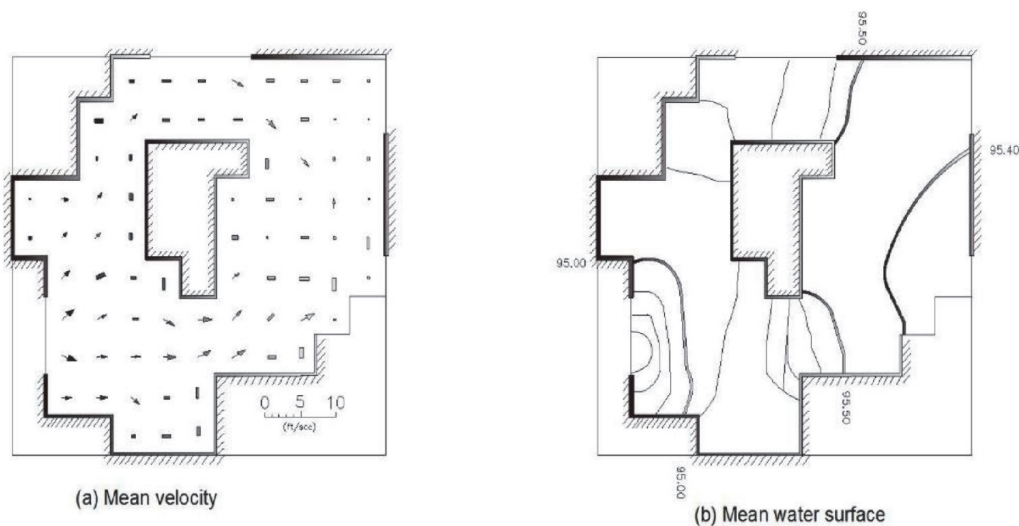*Mean velocity and water surface profiles at 5 h.*

Figure 21.
Mean velocity and water surface profiles at 10 h.

hydrographs. DHM computed flow patterns compare well to a similar study
prepared by Lai [5].

3. Application for channel and floodplain interface model

3.1 Application 7: channel-floodplain model

Figure 22 depicts a discretization of a two-dimensional hypothetical watershed
with three major channels crossing through the flood plain.

Figure 23 depicts the inflow and outflow boundary conditions for the hypothet-
ical watershed model. **Figures 24–30** illustrate the evolutions of the flood plain.

The shaded areas indicate which grid element is flooded. From **Figure 24**, it is
seen that the outflow rates at nodes 31, 71, and 121 are less than the corresponding
inflow rates, which result in a flooding situation adjacent to the outflow grid ele-
ments. The junction of channel B and B′ is also flooded. At the end of the peak
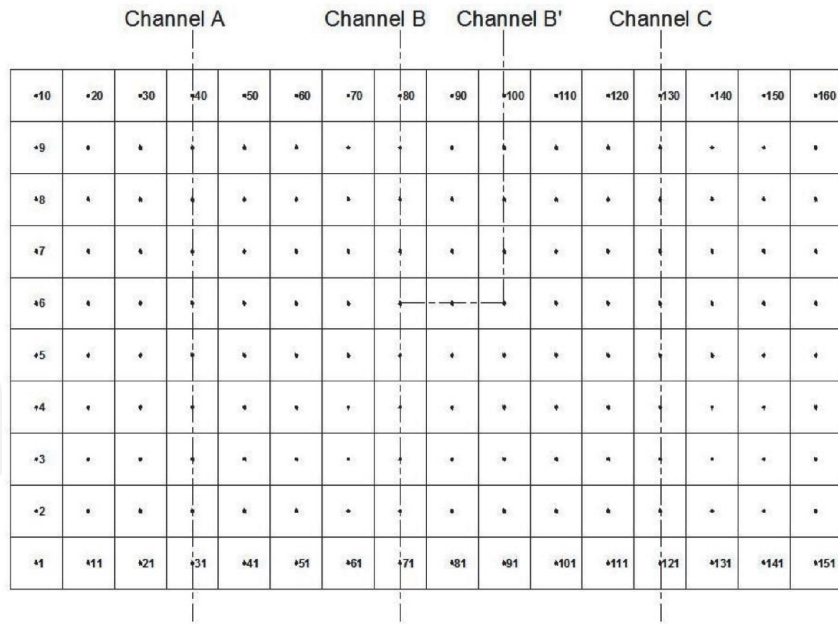
Figure 22.
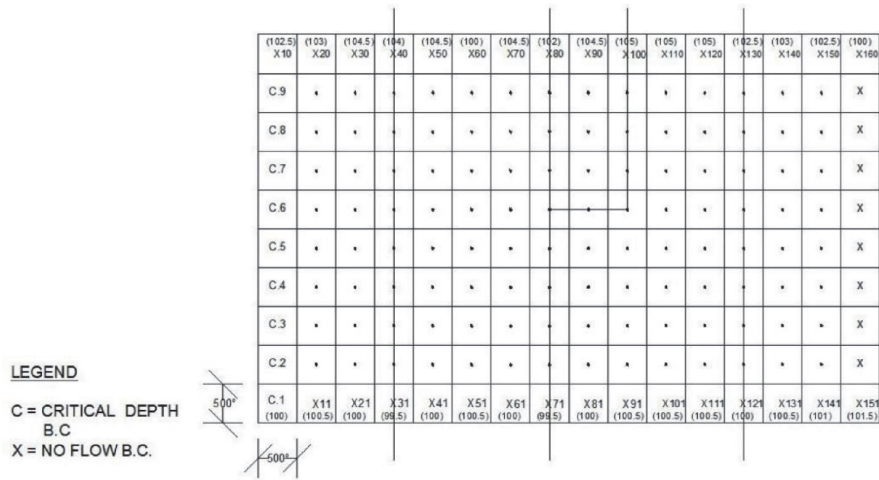*Diffusion hydrodynamic model discretization of a hypothetical watershed model.*

Figure 23.
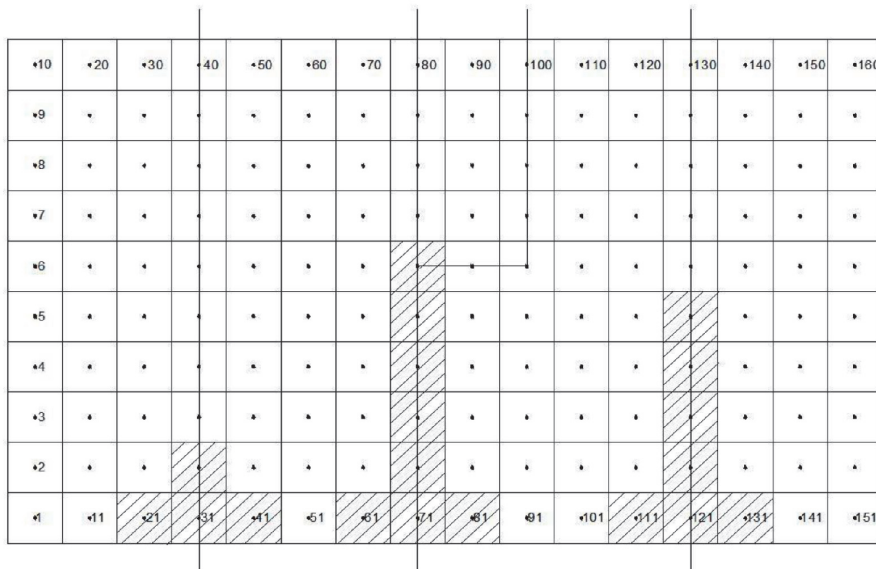*Inflow and outflow boundary conditions for the hypothetical watershed model.*

Figure 24.
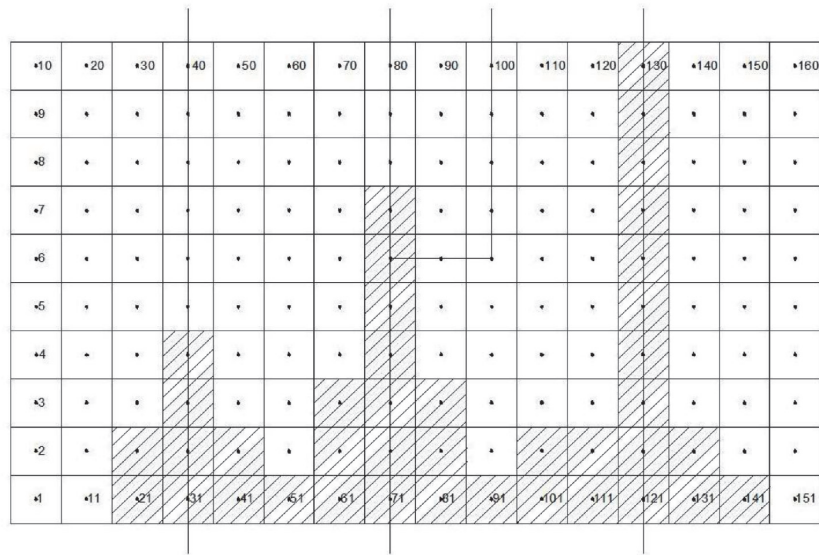*Diffusion hydrodynamic modeled floodplain at time = 1 h.*

16

Figure 25.
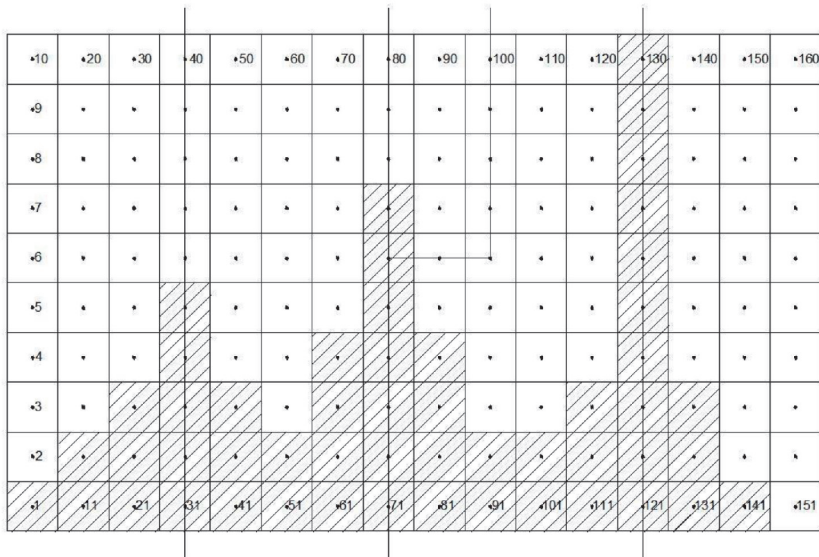*Diffusion hydrodynamic modeled floodplain at time = 2 h.*

Figure 26.
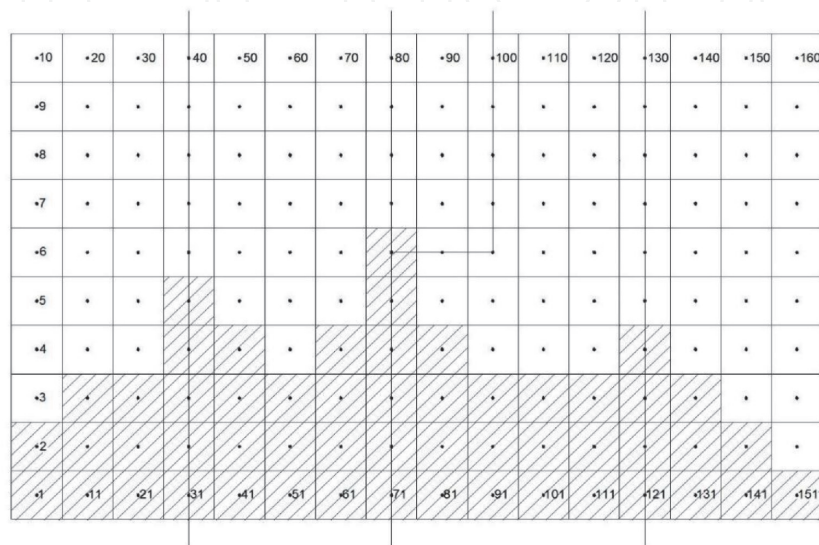*Diffusion hydrodynamic modeled floodplain at time = 3 h.*

Figure 27.
Diffusion hydrodynamic modeled floodplain at time = 5 h.

17

inflow rate (**Figure 26**), about 1/3 of the flood plain is flooded. **Figure 29** indicates a flooding situation along the bottom of the basin after 10 h of simulation. **Figure 30** shows the maximum depth of water at four downstream cross sections. It is needed to point out that the maximum water surface for each grid element is not
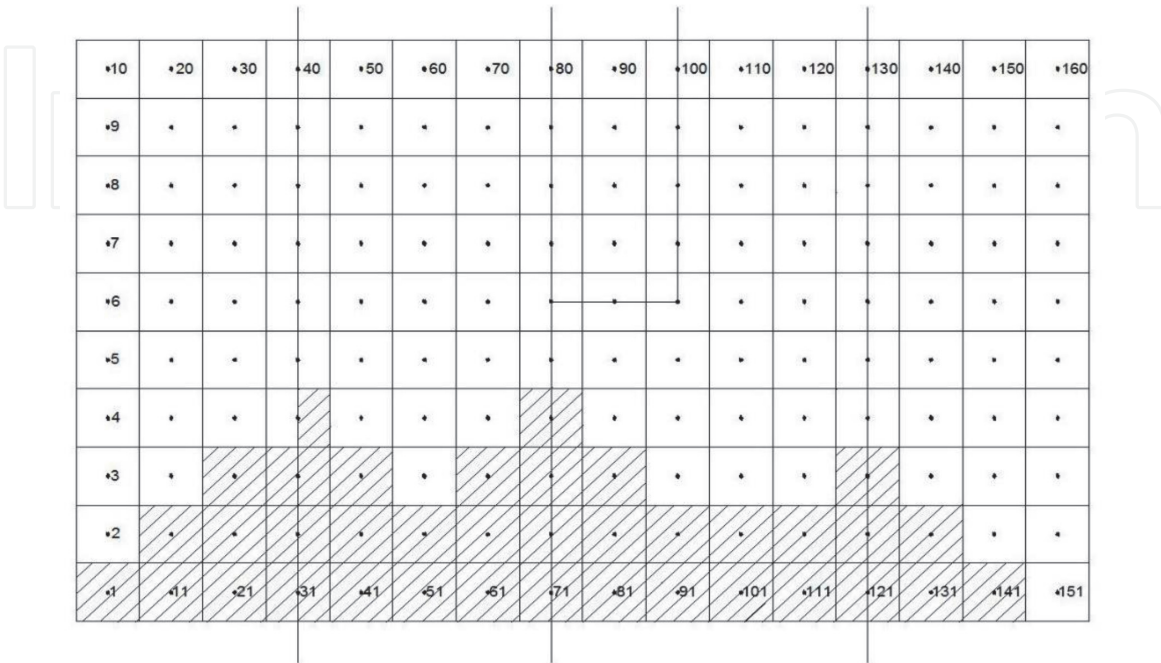

Figure 28.
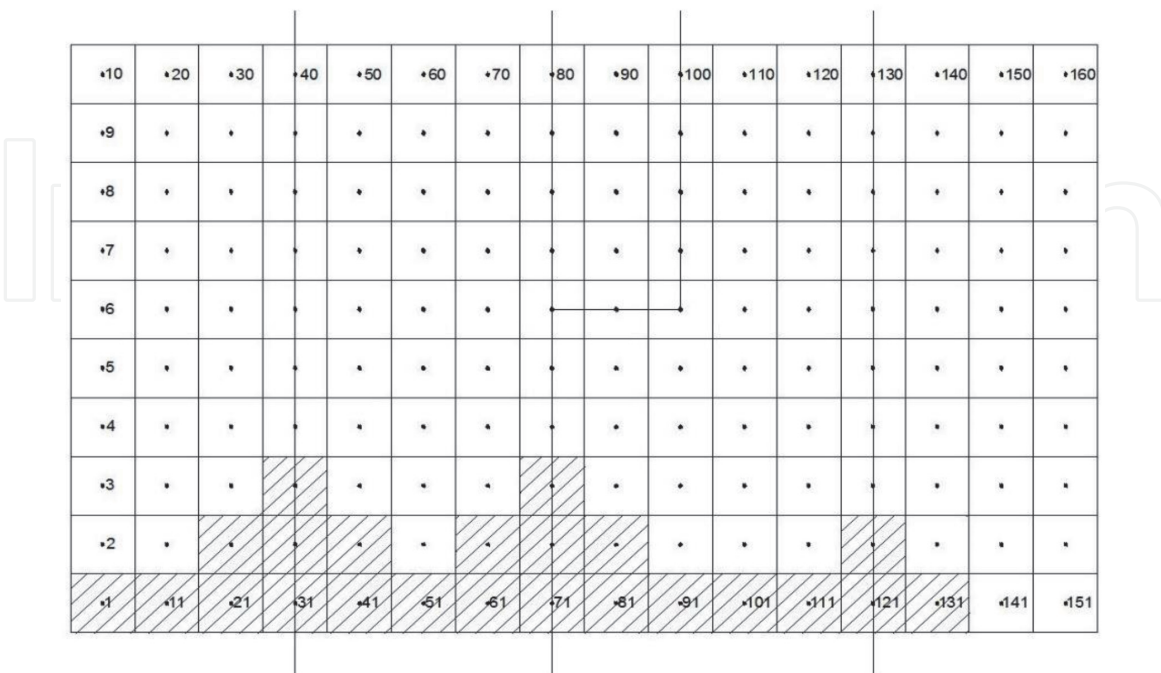*Diffusion hydrodynamic modeled floodplain at time = 7 h.*

Figure 29.
Diffusion hydrodynamic modeled floodplain at time = 10 h.
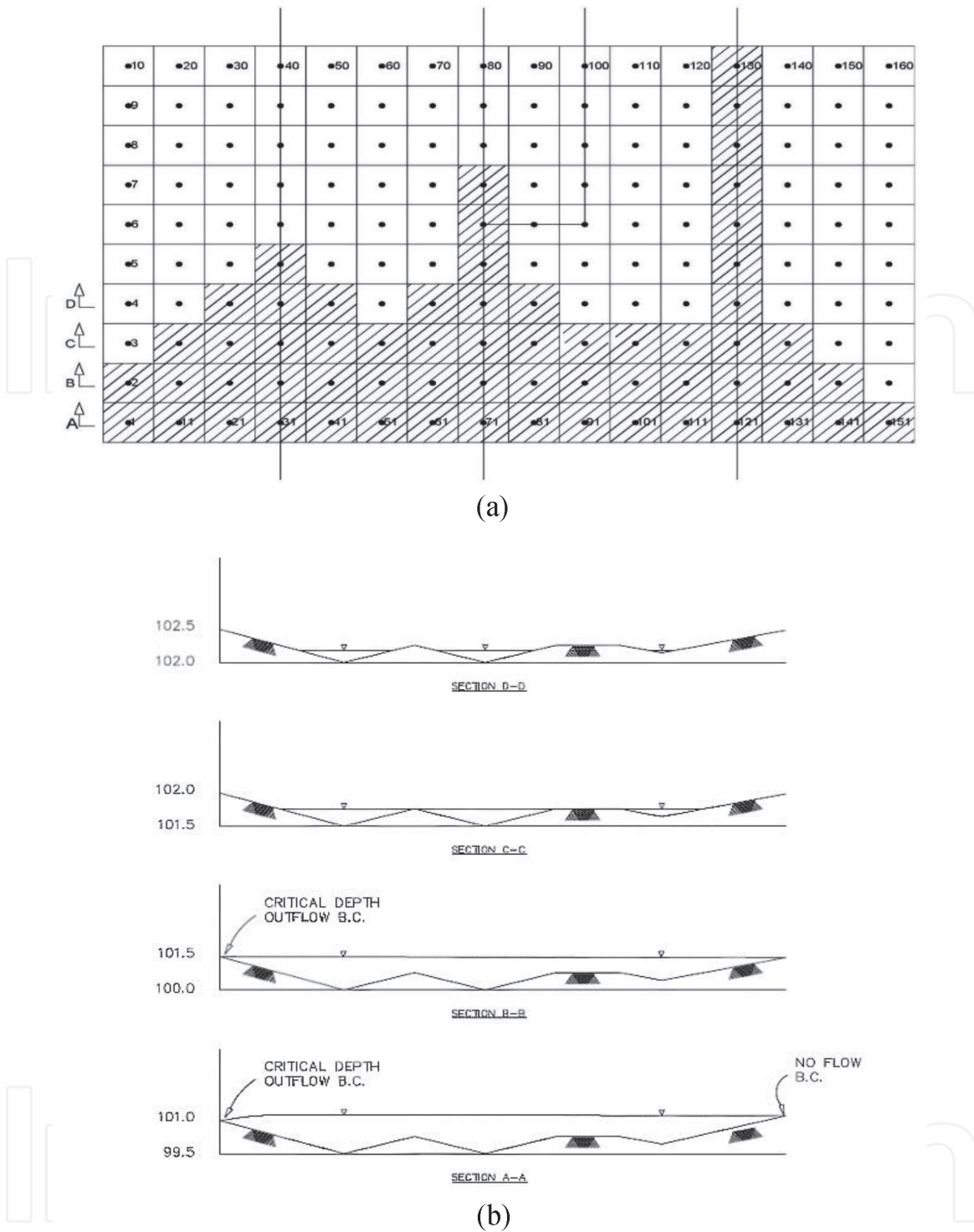
(a)

(b)

Figure 30.
Maximum water depth at different cross sections. (a) Maximum floodplain and (b) maximum water profiles.

necessarily incurred at the same time. Finally, **Figures 31** and **32** depict the outflow hydrographs for both the channel system and the flood plain system.

Until now, no existing numerical model can successfully simulate or predict the evolution of the channel-floodplain interface problem. The proposed DHM uses a simple diffusion approach and interface scheme to simulate the channel-floodplain interface development.
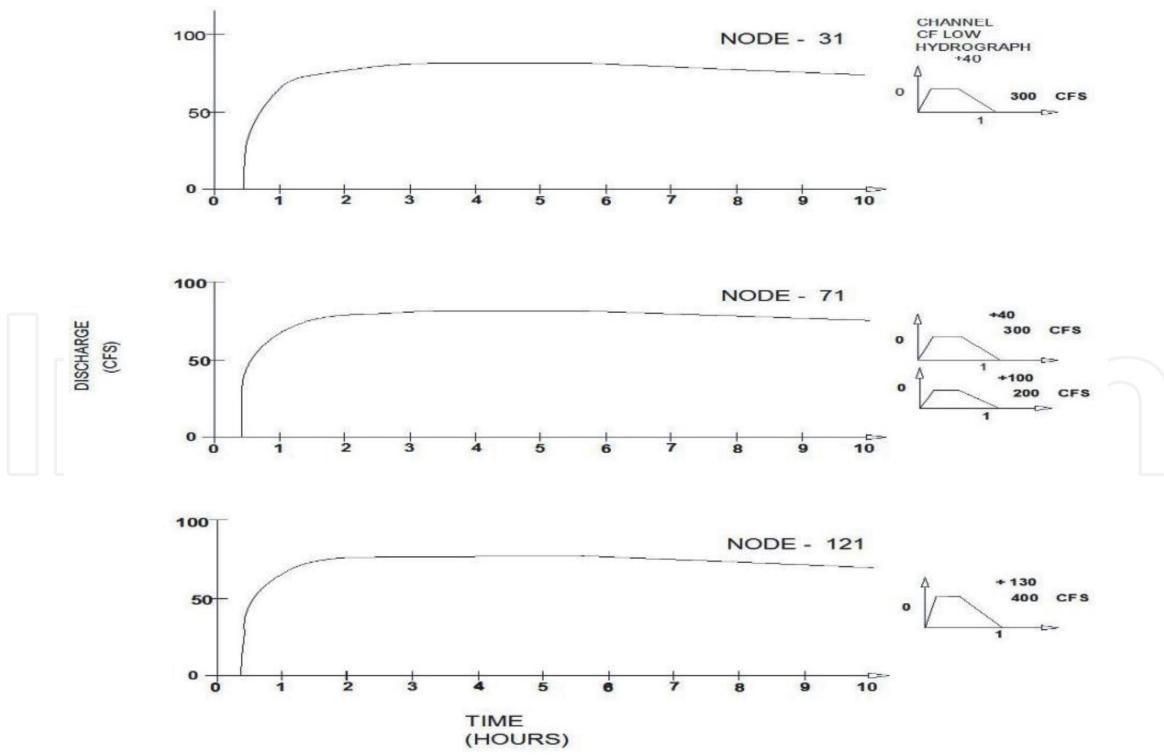
Figure 31.
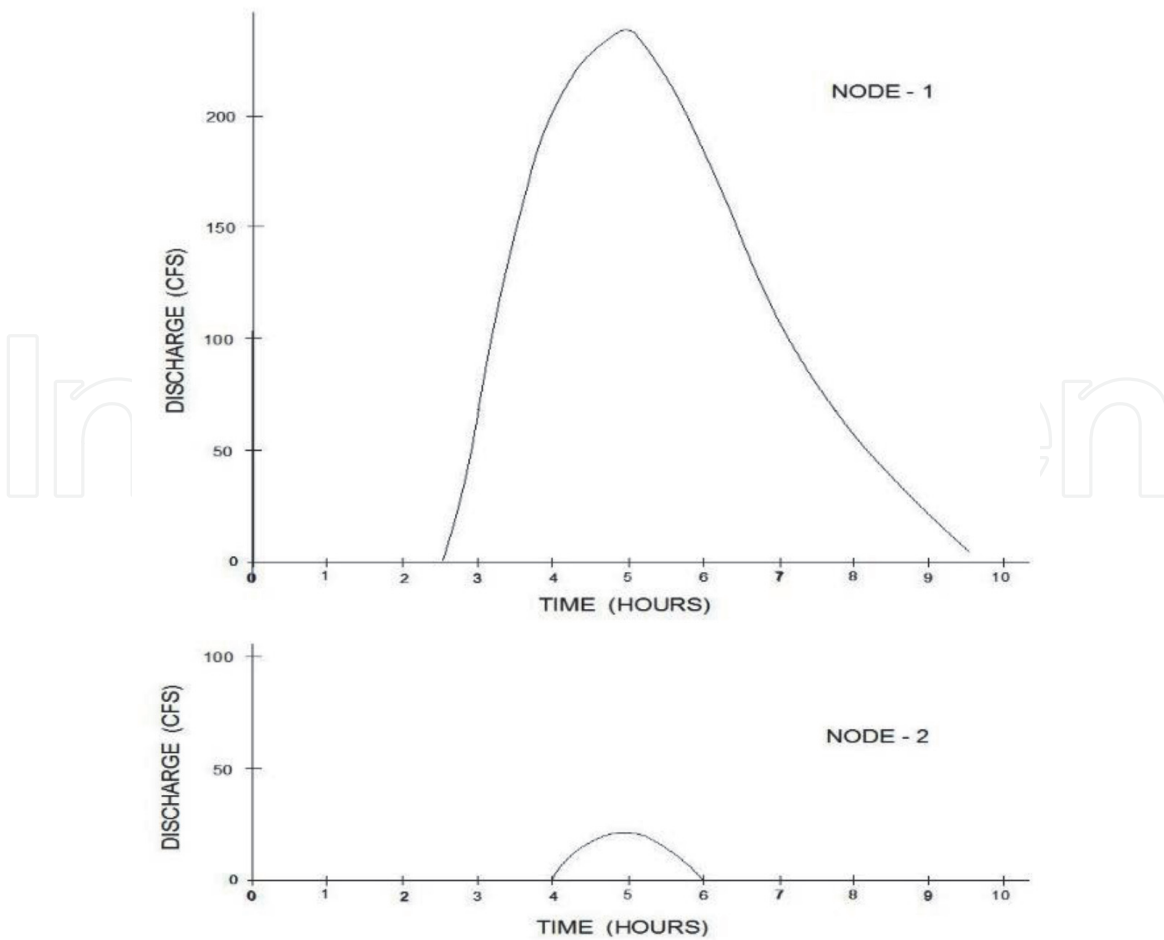*Bridge flow hydrographs assumed outflow relation (Q = 10 d).*

Figure 32.
Critical outflow hydrographs for floodplain.

Author details

Theodore V. Hromadka II[1*] and Chung-Cheng Yen[2]

1 Department of Mathematical Sciences, United States Military Academy,
West Point, NY, USA

2 Tetra Tech, Irvine, CA, USA

*Address all correspondence to: ted@phdphdphd.com

IntechOpen

References

[1] Henderson FM. Open Channel Flow. New York: MacMillan Publishing Co., Inc.; 1966. p. 522

[2] Hromadka TV II, Nestlinger AB. Using a two-dimensional diffusional dam-break model in engineering planning. In: Proceedings: ASCE Workshop on Urban Hydrology and Stormwater Management, Los Angeles County Flood Control District Office. Los Angeles, California; 1985

[3] Hromadka TV II, Lai C. Solving the two-dimensional diffusion flow model. In: Proceedings: ASCE Hydraulics Division Specialty Conference. Orlando, Florida; 1985

[4] Metropolitan Water District of Southern California. Dam-Break Inundation Study for Orange County Reservoir. Los Angeles, California; 1973

[5] Lai C. Computer Simulation of Two-Dimensional Unsteady Flows in Estuaries and Embayments by the Method of Characteristics—Basic Theory and the Formulation of the Numerical Method. Reston, Virginia: U.S. Geological Survey, Water Resources Investigation; 1977. pp. 77-85